Magnetic nanoparticle-based isolation of endocytic vesicles reveals a role of the heat shock protein GRP75 in macromolecular delivery

Anders Wittrup[a], Si-He Zhang[a], Katrin J. Svensson[a], Paulina Kucharzewska[a], Maria C. Johansson[a], Matthias Mörgelin[b], and Mattias Belting[a,1]

Sections of [a]Oncology and [b]Clinical and Experimental Infectious Medicine, Department of Clinical Sciences, Lund University, SE-221 85, Lund, Sweden

An increased understanding of cellular uptake mechanisms of macromolecules remains an important challenge in cell biology with implications for viral infection and macromolecular drug delivery. Here, we report a strategy based on antibody-conjugated magnetic nanoparticles for the isolation of endocytic vesicles induced by heparan sulfate proteoglycans (HSPGs), key cell-surface receptors of macromolecular delivery. We provide evidence for a role of the glucose-regulated protein (GRP)75/PBP74/mtHSP70/mortalin (hereafter termed "GRP75") in HSPG-mediated endocytosis of macromolecules. GRP75 was found to be a functional constituent of intracellular vesicles of a nonclathrin-, noncaveolin- dependent pathway that was sensitive to membrane cholesterol depletion and that showed colocalization with the membrane raft marker cholera toxin subunit B. We further demonstrate a functional role of the RhoA GTPase family member CDC42 in this transport pathway; however, the small GTPase dynamin appeared not to be involved. Interestingly, we provide evidence of a functional role of GRP75 using RNAi-mediated down-regulation of GRP75 and GRP75-blocking antibodies, both of which inhibited macromolecular endocytosis. We conclude that GRP75, a chaperone protein classically found in the endoplasmic reticulum and mitochondria, is a functional constituent of noncaveolar, membrane raft-associated endocytic vesicles. Our data provide proof of principle of a strategy that should be generally applicable in the molecular characterization of selected endocytic pathways involved in macromolecular uptake by mammalian cells.

drug delivery | endocytosis | heparan sulfate | proteoglycan | membrane raft

Endocytosis is the process by which cells compartmentalize constituents of the plasma membrane and the extracellular space into intracellular vesicles for further sorting to specific cellular locations (1–4). Endocytosis regulates signaling events involved in cell motility and cell fate determination and can be exploited by microbial intruders for infection. Interestingly, the same pathways may be used for the delivery of therapeutic macromolecules (e.g., DNA, anti-sense oligonucleotides, and siRNA) in the treatment of various diseases. A more detailed understanding of endocytic mechanisms thus is a major challenge in basic cell biology with implications for viral infection, the regulation of signaling networks in cancer (3), and the development of macromolecular drugs (5).

High-resolution, live-cell imaging techniques have unraveled the heterogeneity of vesicular compartments in terms of kinetic/dynamic parameters as well as ligand specificity. In addition to the classical clathrin-dependent mechanism of endocytosis, several clathrin-independent endocytic pathways are emerging (3, 4, 6). Collectively, published data from several groups indicate that ligands can be taken up by multiple lipid raft-mediated pathways; however, these pathways require further definition at the molecular level. Classification schemes based on the dependence on/association with dynamin, caveolin-1, and the RhoA family GTPases Rac1, RhoA, and CDC42 have been proposed. Caveolae, a dynamin-

dependent pathway involved in the internalization of a diverse set of cargoes (7, 8), share many characteristics with cholesterol- and glycosphingolipid-rich membrane rafts. By using comparative proteomics on detergent-resistant raft membrane preparations from cav-1$^{-/-}$ and wild-type fibroblasts, polymerase I and transcript release factor recently was identified as a constituent involved in caveolae formation (7). Similar approaches have been used to define the anatomy of other trafficking vesicles (9, 10). These findings have contributed profoundly to our understanding of endocytic mechanisms; however, they are limited by their reliance on the fractionation and analysis of detergent-resistant cell-membrane preparations.

Heparan sulfate proteoglycans (HSPGs), a family of proteins substituted with polysulfated heparan sulfate (HS) polysaccharides, have a key role in the endocytic uptake of a diverse set of macromolecular drugs, growth factors, and morphogens (2, 5, 11, 12) with important implications for early developmental patterning and cancer. Here, we have capitalized on the recent finding (13) that magnetic nanoparticles can be endocytosed efficiently by conjugation to a specific, phage-derived anti-HS antibody (αHS) for the isolation and analysis of intact, endocytic vesicles. Our studies reveal a role of the chaperone 75-kDA glucose-regulated protein (GRP75) as a functional constituent of a defined endocytic pathway.

Results

Identification of GRP75 in HSPG-Associated Endocytic Vesicles. We set out to develop a strategy for qualitative analysis of the HSPG-dependent endocytic compartment of macromolecular delivery based on the internalization of single-chain fragment anti-HS–conjugated superparamagnetic nanoparticles (scFv-αHS$_M$). Among several scFv-αHS clones, only one, AO4B08, efficiently delivers magnetic nanoparticles to intracellular vesicles (13). Magnetic separation of mechanically disrupted cells that had internalized scFv-αHS$_M$ yielded a population of intact, scFv-αHS$_M$–containing vesicles (Fig. 1A). Importantly, it has been established that uptake of nanoparticles per se (i.e., in the absence of scFv-αHS) is insignificant, and that internalized scFv-αHS$_M$ and fluorophor-labeled scFv-αHS$_F$ antibody complexes show strong colocalization in endocytic vesicles (13). Moreover, the uptake of scFv-αHS$_F$ as well as scFv-αHS$_M$ was absent in HSPG-deficient cells, indicating that the magnetic nanoparticle does not affect the endocytic route itself and that the uptake of scFv-αHS$_M$ is
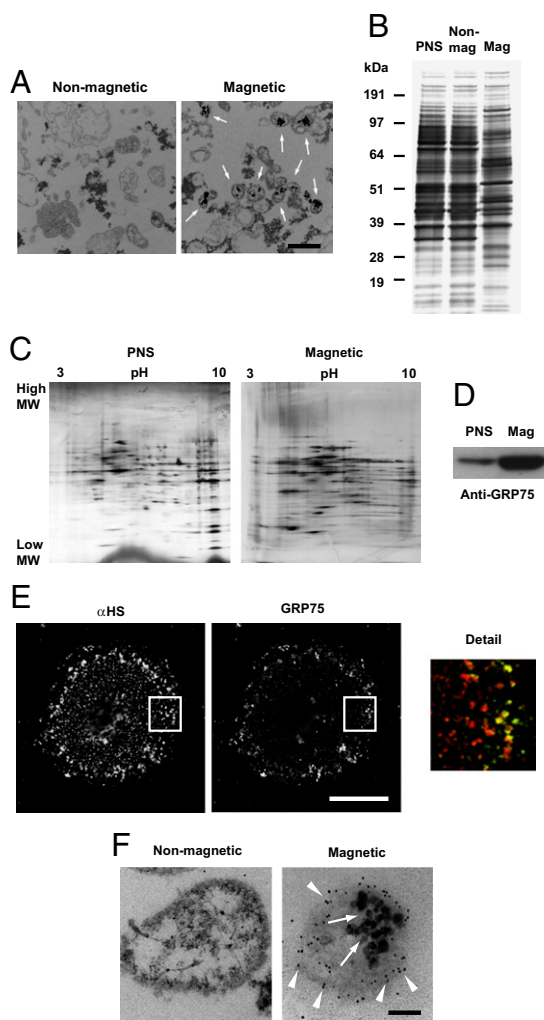
Fig. 1. Identification of GRP75 as a constituent of HSPG-induced endocytic vesicles. (*A*) Localization of superparamagnetic nanoparticles in endocytic vesicles. HeLa cells incubated with scFv-αHS$_M$ were mechanically disrupted, centrifuged to remove cell nuclei and debris to yield a PNS, and separated into a nonmagnetic and a magnetic fraction. Shown are representative electron microscopy images of the respective fractions. Arrows indicate magnetic nanoparticle-loaded endocytic vesicles. (Scale bar, 1 μm.) (*B*) The PNS nonmagnetic (Nonmag) and magnetic (Mag) fractions from the experiment described in *A* were analyzed by 1D gel electrophoresis, showing a distinct pattern of protein bands in the magnetic fraction. (*C*) The enrichment of several protein components in the magnetic fraction as compared with the PNS was revealed further by 2D gel electrophoresis. (*D*) Immunoblotting with anti-GRP75 antibody shows the enrichment of GRP75 in the magnetic fraction as compared with PNS. Equal amounts of total protein were loaded in the two lanes. (*E*) Confocal microscopy shows colocalization of scFv-αHS$_F$ and GRP75 in vesicular structures. (*Detail*) Higher-magnification (×3) image of the indicated areas in left panels; anti-GRP75 staining (green) and scFv-αHS (red). (Scale bar, 10 μm.) (*F*) Immunogold staining for GRP75 and electron microscopy shows the enrichment of GRP75 in magnetically isolated vesicles (*Right*) as compared with vesicles from the nonmagnetic fraction (*Left*). Arrowheads indicate gold particles; arrows indicate magnetic nanoparticles. (Scale bar, 100 nm.)

strictly dependent on HSPG expression (13). In further support of this notion, scFv-αHS$_M$ association with target cells was highly dependent on electrostatic interactions, because high molar NaCl efficiently inhibited cellular binding of scFv-αHS$_M$ (Fig. S1*A*). Moreover, the uptake was unperturbed in the presence of up to 5% serum (Fig. S1*B*).

The protein composition of isolated vesicles and postnuclear cell lysates was compared by 1D and 2D gel electrophoresis,

showing the enrichment of several proteins in the vesicular preparation (Fig. 1 *B* and *C*). We decided to focus on one of these proteins, the heat shock protein (HSP) family member GRP75 that consistently appeared as one of the dominating vesicular components, as determined by MALDI-TOF and LC-MS/MS. Previous studies have suggested that GRP75 (also known as "PBP74") not only is present in the endoplasmic reticulum (ER) but also is associated with the plasma membrane and in early endocytic vesicles in immune cells, suggesting a role in antigen processing (14). Others have reported on cytosolic localization of GRP75 (also known as "mortalin"), where it may regulate the activity of p53 (15) and FGF (16). More recent proteomic analyses of detergent-resistant membrane fractions have suggested GRP75 is a ubiquitously expressed membrane lipid raft protein (17); however, the role of GRP75 in endocytic mechanisms remains unknown. MS data were confirmed by immunoblotting experiments, showing substantial enrichment of GRP75 in endocytic vesicles (Fig. 1*D*). These data were corroborated by confocal microscopy, showing the localization of GRP75 to scFv-αHS–induced vesicular compartments in intact cells (Fig. 1*E*). Importantly, immunogold staining and electron microscopy showed the enrichment of GRP75 in magnetically isolated vesicles (Fig. 1*F*). The fact that both scFv-αHS$_M$ and scFv-αHS$_F$ colocalized with GRP75 provides additional evidence that the nanoparticle per se has no significant impact on the endocytic route. To address further whether GRP75 is located inside or at the surface of isolated vesicles, trypsin-treated and untreated vesicles were analyzed for GRP75 levels. As shown in Fig. S1*C*, GRP75 remained virtually intact after trypsin treatment. Notably, cell-surface GRP75 was shown to be highly trypsin sensitive (see cell-surface biotinylation experiments below). As a positive control, we found efficient degradation by trypsin of the cytoskeleton proteins actin and tubulin that are associated with the surface of endocytic vesicles (Fig. S1*C*). Together, these data indicate that GRP75 is a genuine resident of endocytic vesicles.

Immunoprecipitation of cell lysates with anti-GRP75 antibody or scFv-αHS did not result in coimmunoprecipitation of HSPG or GRP75, respectively. Moreover, GRP75 showed no specific binding to heparin Sepharose (Fig. S2). These results suggest that although GRP75 and HSPG colocalize in endocytic vesicles, they do not interact directly.

Characterization of the GRP75-Associated Endocytic Pathway. We next performed studies with fluorophor-labeled scFv-αHS$_F$ antibody complexes to define the GRP75-associated endocytic pathway. As shown in Fig. 2*A*, scFv-αHS uptake was highly sensitive to membrane cholesterol depletion by β-methyl-cyclodextrin (MCD). In similar experiments, transferrin uptake was intact or even upregulated, whereas uptake of the membrane raft marker cholera toxin subunit B (CTxB) was substantially inhibited (Fig. 2*A*), indicating that cholesterol depletion preferentially inhibited nonclathrin-dependent endocytosis under these conditions.

The scission of clathrin-dependent, caveolae-dependent as well as some, but not all, additional raft-associated vesicles has been shown to depend on dynamin GTPase activity (3). As expected, the expression of dominant-negative dynamin substantially decreased clathrin-dependent transferrin uptake; however, dynamin inhibition had no significant effect on the uptake of scFv-αHS$_F$ (Fig. 2*B*). Moreover, there was no significant colocalization of scFv-αHS–positive vesicles and the fluid-phase uptake marker dextran (Fig. S3*A*), whereas scFv-αHS$_F$ showed strong colocalization with the membrane raft marker CTxB (Fig. 2*C*).

Caveolae-dependent endocytosis is one the most studied clathrin-independent pathways (8) and shares many characteristics with membrane lipid rafts. Internalized scFv-αHS$_F$ showed no colocalization with either endogenous caveolin-1 or ectopically expressed caveolin-1-YFP (Fig. 2D and Fig. S3*B*). Accordingly, flow cytometry analysis of the postnuclear supernatant (PNS) from caveolin-1-YFP–expressing cells incubated with scFv-αHS$_F$
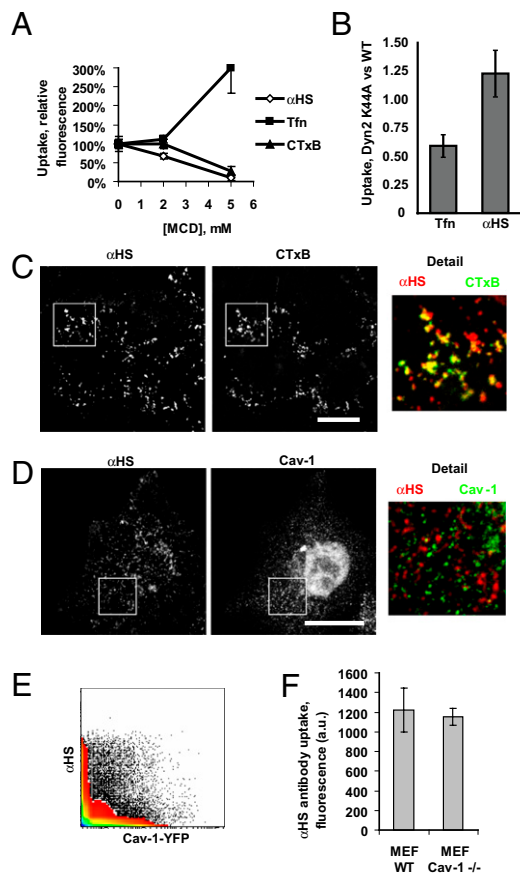
Fig. 2. GRP75 is associated with nonclassical endocytosis. (A) Cholesterol depletion in HeLa cells by MCD dose-dependently inhibited the uptake of scFv-αHS$_F$ and the membrane raft marker CTxB, whereas clathrin-dependent uptake of transferrin (Tfn) was unaffected (2 mM MCD) or even increased (5 mM MCD). (B) Inhibition of dynamin activity in HeLa cells reduced the uptake of transferrin (Tfn), as expected, whereas scFv-αHS$_F$ uptake was unperturbed. (C and D) ScFv-αHS$_F$ colocalizes with CTxB but not with caveolin-1–associated vesicles, as determined by confocal microscopy. (Details) Higher-magnification (×3) images of the indicated areas in left panels. (Scale bars, 10 μm.) (E) Flow cytometry sorting of PNS from stable caveolin-1-YFP HeLa cell transfectants incubated with scFv-αHS$_F$ shows separation of scFv-αHS$_F$– and caveolin-1-YFP (Cav1-YFP)–positive particles into two distinct populations. Experimental details are provided in *Materials and Methods*. (F) Wild-type and caveolin-1$^{-/-}$ MEFs displayed no significant difference in the uptake of scFv-αHS$_F$.

separated caveolin-1-YFP– and scFv-αHS$_F$–positive particles into two distinct populations (Fig. 2E). Moreover, scFv-αHS$_F$ uptake was unperturbed in caveolin-1$^{-/-}$ cells as compared with wild-type control cells (Fig. 2F).

Together, the data indicate that GRP75 is associated with an endocytic pathway characterized by the independence of caveolin and dynamin, by the sensitivity to cholesterol depletion, and by colocalization with the membrane raft marker CTxB. These findings prompted further studies on the involvement of CDC42, a small GTPase that has been implicated specifically in noncaveolar, dynamin-independent, raft-mediated endocytosis (3, 18). Interestingly, scFv-αHS significantly induced the fraction of active, GTP-bound CDC42 in a time-dependent manner (Fig. 3A). However, another scFv-αHS clone, EV3C3, that is known to bind to but is not internalized by HeLa cells (13), did not significantly induce CDC42-GTP (Fig. S4). Using wild-type CDC42 (EGFP-CDC42, WT) and dominant-negative (EGFP-CDC42, T17N) HeLa cell transfectants, a functional role of CDC42 was suggested by confocal microscopy analysis (Fig. 3B); flow cytometry analysis of trypsinized
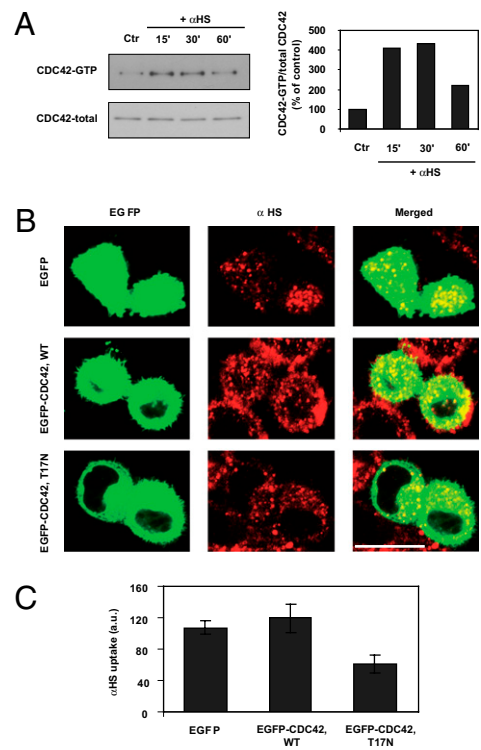

Fig. 3. GRP75-associated endocytosis is defined by the dependence on the small GTPase CDC42. (A) (Left) ScFv-αHS induces CDC42 activity. HeLa cells were untreated (Ctr) or stimulated with scFv-αHS (AO4B08) for the indicated time periods, followed by immunoblotting for GTP-bound CDC42 and total CDC42. (Right) Ratios of GTP-bound CDC42 vs. total CDC42 in control and scFv-αHS–treated cells from a representative experiment. (B and C) CDC42 inhibition reduces HSPG-induced endocytosis. HeLa cells transfected with GFP control plasmid (EGFP), EGFP-CDC42, WT or dominant-negative EGFP-CDC42, T17N plasmid were incubated with scFv-αHS$_F$ (red) and analyzed by confocal microscopy (B) and by flow cytometry (C), following trypsinization, as described in *Materials and Methods*. (Scale bar, 20 μm.)

cells confirmed that scFv-αHS$_F$ uptake was reduced by almost half in EGFP-CDC42, T17N-expressing cells as compared with EGFP-CDC42, WT and EGFP-transfected control cells (Fig. 3C).

Functional Role of GRP75 in Endocytosis. The above data identify GRP75 as a constituent of endocytic vesicles of a defined pathway. We next set out to investigate the functional role of GRP75 in endocytosis. Interestingly, RNAi-mediated down-regulation of GRP75 resulted in an approximately 50% inhibition of scFv-αHS$_F$ uptake as compared with untransfected control cells or cells transfected with scrambled siRNA (Fig. 4A, black bars). The amount of cell-surface HSPG, as determined by cell association of scFv-αHS$_F$ at 4 °C, was unaffected by GRP75 down-regulation (Fig. 4A, white bars). Moreover, treatment with an anti-GRP75 antibody dose-dependently inhibited endocytosis of scFv-αHS$_F$ (up to approximately 50% inhibition as compared with untreated control; Fig. 4B, black bars). However, cell-surface binding of scFv-αHS$_F$ was unaffected by anti-GRP75 antibody (Fig. 4B, white bars). Also, treatment with a control IgG antibody had no significant effect on scFv-αHS$_F$ uptake (Fig. S5). These results indicate that the inhibitory effects on scFv-αHS$_F$ uptake by GRP75 knockdown and anti-GRP75 antibody are not a result of disturbed intracellular sorting, recycling, or cell-surface localization of HSPG or of direct interference with scFv-αHS$_F$ binding to cell-surface HSPG. The finding that inhibition of GRP75 significantly decreased the uptake of CTxB (Fig. 4C, white bars) but not the uptake of clathrin-dependent transferrin uptake (Fig. 4C, black bars) suggests a more general role of GRP75 in nonclassical endocytosis.
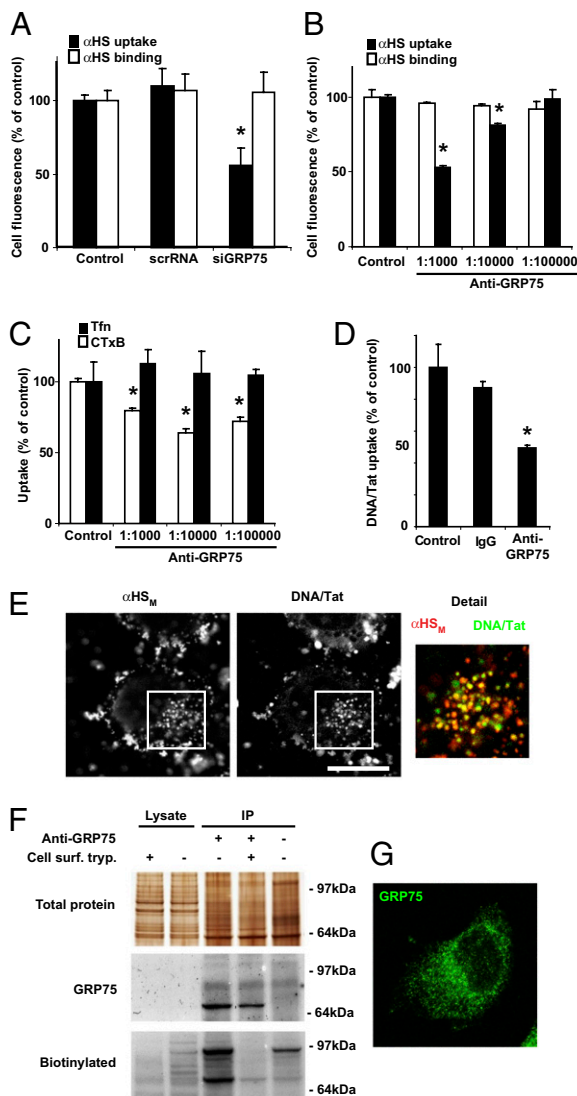
www.manaraa.com

Fig. 4. GRP75 has a functional role in endocytosis. GRP75 siRNA and anti-GRP75 antibody inhibit endocytosis. (A) HeLa cells, untransfected (Control) or transfected with a scrambled siRNA sequence (scrRNA) or siRNA directed at GRP75 mRNA (siRNA-GRP75) were analyzed for scFv-αHS$_F$ uptake at 37 °C (black bars) and scFv-αHS$_F$ cell-surface binding at 4 °C (white bars). Efficient knock-down of GRP75 mRNA and protein by siRNA-GRP75 (approximately 90% reduction as compared with Control and scrRNA) are shown in Fig. S7. (B) HeLa cells were analyzed for the uptake and binding of scFv-αHS$_F$ as in A either in the absence (Control) or in the presence of the indicated titers of anti-GRP75 antibody. (C) Treatment with anti-GRP75 antibody at titers similar to those in B shows substantial inhibition of the uptake of the membrane raft marker CTxB, whereas Tfn uptake is virtually unaffected. As a control of the data shown in B and C, similar experiments were performed with an isotype-matched IgG antibody, showing no effect on scFv-αHS, CTxB, or Tfn uptake (Fig. S5). (D) HeLa cells were incubated with Tat peptide (10 μg/mL) precomplexed with YOYO-1-labled DNA (2 μg/mL), either in the absence (Control) or in the presence of anti-GRP75 antibody (1:10,000) for 1 h at 37 °C, and Tat-mediated DNA uptake was determined in trypsinized cells by flow cytometry. As an additional control, Tat-DNA complex uptake was performed in the presence of an isotype-matched IgG antibody. *Statistically significant inhibition as compared with control; $P < 0.01$. (E) HeLa cells were coincubated with fluorescent scFv-αHS$_M$ containing Cy3-coupled mouse anti-vesicular stomatitis virus glycoprotein (VSV) and Tat-DNA complexes, prepared as described in D for 2.5 h at 37 °C and then were analyzed using confocal microscopy. (Scale bar, 10 μm.) (Detail) Higher-magnification (×2) image of the indicated areas in left panel. (F) Cell-surface localization of GRP75. HeLa cells were cell-surface biotinylated with a membrane-impermeable biotinylation reagent and then lysed with detergent with or without prior removal of trypsin-sensitive cell-surface proteins by trypsin treatment. Cell lysates (Ly-

The HIV-TAT–derived transduction peptide, Tat, is a well-known cell-penetrating peptide (CPP) previously shown to mediate DNA uptake in HSPGs (19). Consistent with a more general role of the GRP75-dependent endocytic pathway in macromolecular delivery, GRP75 inhibition reduced cellular uptake of CPP-DNA complexes, and scFv-αHS$_M$ colocalized with CPP-DNA complexes in vesicles (Fig. 4 D and E). Further, basic fibroblast growth factor (bFGF), a well-known, nonnanoparticle ligand of HSPGs (20, 21), coassociated with scFv-αHS in endocytic vesicles, and bFGF internalization was significantly inhibited by scFv-αHS (Fig. S6).

Finally, the fact that blocking GRP75 inhibited endocytic uptake of macromolecules prompted us to investigate possible cell-surface localization of GRP75. Indeed, a fraction of GRP75 was accessible at the extracellular part of the plasma membrane, as shown by cell-surface biotinylation experiments (Fig. 4F); accordingly, nonpermeabilized cells showed a multifocal cell-surface staining for GRP75 (Fig. 4G).

Discussion

This study provides evidence for a role of the HSP70 family member GRP75 in a defined endocytic pathway involving macromolecular uptake through cell-surface HSPGs. In fact, relatively few endogenous, noncargo proteins involved in nonclassical endocytic pathways have been identified (3), and little is known about their functional role in membrane transport of exogenous ligands. The fact that extraction of cell membranes with cold, nonionic detergents (e.g., triton) generates a cholesterol-rich membrane fraction enriched in specific proteins has led to the general assumption that membrane rafts can be captured as detergent-resistant membrane rafts. Thus, alternative strategies to identify specific proteins and lipids involved in endocytosis present an important challenge.

The various names given to GRP75 reflect the multifunctional nature of the protein [i.e., the regulation of the glucose response in rats (GRP75), the involvement in antigen-processing in mice (PBP74), the mitochondrial protein transport pathway in humans (mtHSP70), and in-cell mortality in mice (mortalin)] (22). Chaperone proteins, including the HSPs, long were thought to be located solely in intracellular compartments, because they do not contain a consensual secretory signal peptide (23); however, more recent studies have documented their presence on the surface of malignant cells where they may stimulate receptor-mediated functions (24–26); for example, cytosolic HSP70 was shown to be released via exosomes in an endolysosomal-dependent pathway (27) or through translocation to the plasma membrane, followed by its release in a membrane-associated form to the extracellular space (28). It has been suggested that cytosolic HSPs in malignant cells may exist in an alternate form at the genetic or transcriptional level, resulting in HSP synthesis through the ER-Golgi secretion pathway (29–31). In support of this notion, HSPs were found to be substituted with sialylated glycans that appear on cell-surface resident and secreted glycoproteins (32).

We demonstrate the presence of GRP75 at the cell surface as well as its enrichment in endocytic vesicles and provide evidence for a functional role of GRP75 in HSPG ligand-induced vesicular

sate) then were separated on SDS gel either directly or after immunoprecipitation (IP) with anti-GRP75 antibody (+) or, as a control, pure protein A-Sepharose beads (−). (Top) Total protein was visualized by silver gel staining. (Middle) Immunoblotting with anti-GRP75 antibody. (Bottom) Immunoblotting with streptavidin-HRP to visualize biotinylated proteins specifically shows a strong band at the position of GRP75 that is absent in cell-surface trypsinized cells. The upper band just below the marker of 97 kDa appears to be a biotinylated, trypsin-sensitive protein that binds nonspecifically to protein A Sepharose beads. (G) Confocal microscopy shows multifocal cell-surface staining for GRP75 in intact, nonpermeabilized HeLa cells.

Wittrup et al.

CELL BIOLOGY

transport of nanoparticles through CDC42-dependent, membrane raft endocytosis. Importantly, we provide data strongly suggesting that this endocytic pathway is not restricted to nanoparticle payload: (*i*) both scFv-αHS$_F$ and scFv-αHS$_M$ colocalized with GRP75 in endocytic vesicles; (*ii*) Tat-DNA complexes colocalized with scFv-αHS$_M$, and GRP75 inhibition reduced the uptake of scFv-αHS$_F$, Tat-DNA complexes as well as that of the membrane raft marker CTxB; and (*iii*) bFGF colocalized with scFv-αHS$_F$, and its uptake was inhibited by scFv-αHS. As an HSP70 family member, GRP75 generally is assumed to regulate protein folding and transmembrane transport of multiprotein complexes. The main function of GRP75 and related chaperones in endocytosis thus may be to facilitate protein–protein interactions at a fundamental level in cholesterol-rich membrane regions, thereby aiding in membrane deformation, in the recruitment of other participating proteins, or by providing a scaffold during the endocytic process. The exact function of GRP75 in vesicle formation or release remains to be clarified in future studies.

We have developed a strategy for proteomic analysis of intact endocytic vesicles, based on the conjugation of an internalizing scFv-αHS (AO4B08) with superparamagnetic nanoparticles. This particular antibody recognizes a specific, 2-O-sulfated iduronic acid-containing HS epitope that appears unique in its ability to induce HSPG-dependent macromolecular uptake through oligomerization or clustering of cell-surface HSPG (13). However, the AO4B08 HS epitope was not associated with a specific HSPG core protein, because members of both the glypican and syndecan families were able to mediate macromolecular uptake (13).

In a previous study (33), ferro-fluid–based magnetic purification of endosomes showed that flotillin-1, or reggie-2, was associated with endosomes that share many characteristics with the pathway described in the present study (i.e., the independence from clathrin, caveolin, and dynamin, and the association with CTxB uptake). Whereas the study by Nichols and coworkers (33) was based on magnetic isolation of vesicles generated by ligand-independent uptake of magnetic water-based dextran fluid with cells in suspension, our studies are based on the isolation of anti-HS antibody-induced vesicles from adherent cells. We did not observe significant enrichment of flotillin-1 in GRP75-enriched vesicles or colocalization of scFv-αHS with flotillin-1 in endosomes, perhaps suggesting differential sorting of nonconjugated and scFv-αHS–conjugated magnetic particles to flotillin-1– and GRP75-associated pathways. This speculation clearly needs to be challenged by further studies directly comparing vesicles from ligand-induced and ligand-independent ferro-fluid uptake in adherent and suspension cells.

In summary, this study presents a role of GRP75 in HSPG-mediated endocytosis of macromolecules and provides a strategy using magnetic nanoparticles that may be applied to characterize specific endocytic pathways involved in the uptake of diverse ligands at the molecular level.

Materials and Methods

Materials are listed in *SI Materials and Methods*.

Cell Culture. Human cervix adenocarcinoma (HeLa) cells and wild-type, and caveolin-1 knock-out mouse embryonal fibroblasts (MEF WT and cav1$^{-/-}$) were from the American Type Culture Collection. HeLa and MEF cells were routinely cultured in a humidified 5% CO_2 incubator at 37 °C, using DMEM supplemented with 10% FBS, 2 mM L-glutamine, 100 U/mL penicillin, and 100 μg/mL streptomycin.

Magnetic Vesicle Purification. αHS (AO4B08, titer 1:40), mouse anti-VSV (1:500), and magnetic MagCellect goat anti-mouse (1:20) antibodies were allowed to form complexes (scFv-αHS$_M$) in DMEM at 20 °C for 30 min. scFv-αHS$_M$ then was added to HeLa cells at 37 °C for 1 h, followed by washing with PBS, trypsin detachment, suspension in DMEM 10% FBS, and washing with PBS. Complete protease inhibitor (Roche) was included in all subsequent steps. Cells then were disrupted mechanically by passage through a 27-G needle during 25 strokes. Remaining intact cells, cell debris, and

nuclei were removed by centrifugation at 500 × *g* for 5 min. The resulting supernatant was pooled with the supernatant obtained after a second centrifugation at 300 × *g* for 3 min to yield a postnuclear supernatant (PNS), which was separated into a magnetic and nonmagnetic fraction using a magnetic separator (PickPen; Bio-Nobile). Protein amounts were quantified using an EZQ kit (Invitrogen). Proteins were separated by 1D gel electrophoresis in a 4–12% NuPAGE gel (Invitrogen) or by 2D gel electrophoresis in 10% 2D-NuPAGE gels (Invitrogen) after 1D separation in a pH 3–10 IPG-strip (SERVA) according to the manufacturer's protocol.

Immunoblotting, heparin affinity chromatography, and electron microscopy experiments are described in *SI Materials and Methods*.

Confocal Fluorescence Microscopy. AO4B08 (titer 1:40), mouse anti-VSV (1:500), and Alexa Fluor (AF)633-conjugated goat anti-mouse (1:100) antibodies were allowed to form complexes (scFv-αHS$_F$) in serum-free DMEM at 20 °C for 30 min. HeLa cells grown in chamber slides then were incubated with scFv-αHS$_F$ at 37 °C for 30 min alone or together with 10 μg/mL FITC-labeled CTxB (Sigma) or rabbit anti-GRP75 (1:100) complexed with AF488 goat anti-rabbit antibodies (1:100). Cells then were rinsed with 1 M NaCl, 0.1 M glycine, pH 2.8, to remove surface-associated ligands. Cells were fixed in 4% (wt/vol) paraformaldehyde and permeabilized with 0.1% Triton-X100. In another series of experiments, HeLa cells were incubated with scFv-αHS$_F$ for 30 min, cell-surface rinsed, fixed, and permeabilized. Cells then were stained with rabbit anti-caveolin-1 (1:200; Abcam) followed by goat anti-rabbit-AF488 antibody (1:500). To visualize cell-surface GRP75 in unperturbed cells, cells were fixed in 4% (wt/vol) paraformaldehyde, stained with rabbit anti-GRP75 (1:500), followed by AF488-conjugated goat anti-rabbit antibody (1:100). All cells were mounted in Permafluor (Beckman Coulter) and analyzed using Zeiss LSM710 confocal scanning equipment with a 63× 1.4NA immersion oil objective.

Flow Cytometry. For antibody binding, cells were detached with PBS (2×)/0.5 mM EDTA, washed with PBS BSA (1% wt/vol), and incubated with αHS (titer 1:20), then washed in PBS BSA and incubated with mouse anti-VSV antibody (1:500), followed by rinsing in PBS BSA and incubation with goat anti-mouse-AF488 antibody (1:200). All antibody incubations were performed in PBS BSA for 30 min on ice. Finally, cells were washed in PBS BSA and analyzed by flow cytometry on a FACSCalibur instrument integrated with Cell-Quest software (BD Biosciences). For uptake experiments, αHS (1:20), mouse anti-VSV (1:500), and goat anti-mouse-AF488 antibodies (1:200) were precomplexed in serum-free medium at 20 °C for 30 min (scFv-αHS$_F$) and then incubated with cells at 37 °C for 1 h. Cells then were trypsinized, suspended in DMEM 10% FBS, washed in PBS BSA, and analyzed by flow cytometry. Controls without αHS primary antibody were included in all experiments.

In some experiments cells were pretreated for 30 min with β-methyl-cyclodextrin (MCD) (Sigma) before uptake of αHS, transferrin-FITC (25 μg/mL) (Sigma), or CTxB-FITC (10 μg/mL) (Sigma) was assayed. In another set of experiments, αHS binding and uptake were measured after αHS coincubation with rabbit polyclonal anti-GRP75 antibody (1:1,000–1:100,000) or equal amounts of control protein, rabbit nonimmune IgG (designated as 1:1,000–1:10,0000) (Sigma). In knockdown experiments, HeLa cells were transfected with GRP75-specific predesigned siRNA (Ambion) or scrambled control siRNA (Ambion) with Lipofectamine 2000 according to the manufacturer's instructions. Knockdown efficiency was assessed using immunoblot and quantitative real-time PCR.

For dynamin 2 dominant-negative experiments, HeLa cells were cotransfected with EGFP and HA-dyn2-WT (1:5) or with EGFP and HA-dyn2-K44A (1:5) using Lipofectamine 2000 (Invitrogen) and were cultured for another 36–48 h to allow plasmid gene expression. ScFv–αHS$_F$ uptake was determined in transfected versus nontransfected cells by flow cytometry through gating of GFP-expressing and -nonexpressing cells. In the case of CDC42 dominant-negative overexpression, αHS uptake was compared in cells transfected either with wild-type EGFP (EGFP-CDC42, WT) or dominant-negative variant of CDC42 (EGFP-CDC42, T17N) (kindly provided by Klaus Hahn, University of North Carolina, Chapel Hill, NC).

Vesicle Detection by Flow Cytometry. HeLa cells stably expressing caveolin-1-YFP were incubated for 1 h with scFv-αHS$_F$, extensively trypsinized, and mechanically disrupted as described to yield a fluorescent PNS. The PNS fraction then was analyzed using a FACSAria cell sorter (BD Biosciences) with the ND FSC filter removed to allow detection of small particles.

Cell-surface biotinylation and immunoprecipitation experiments are described in *SI Materials and Methods*.

Statistical Analyses. Microscopy, flow cytometry, and gel electrophoresis data are representative of at least three independent experiments. Data points in flow cytometry experiments are the mean ± SD (*n* = 3).

Wittrup et al.

www.manaraa.com

1. Lakadamyali M, Rust MJ, Zhuang X (2006) Ligands for clathrin-mediated endocytosis are differentially sorted into distinct populations of early endosomes. *Cell* 124: 997–1009.
2. Belting M, Sandgren S, Wittrup A (2005) Nuclear delivery of macromolecules: Barriers and carriers. *Adv Drug Deliv Rev* 57:505–527.
3. Mayor S, Pagano RE (2007) Pathways of clathrin-independent endocytosis. *Nat Rev Mol Cell Biol* 8:603–612.
4. Conner SD, Schmid SL (2003) Regulated portals of entry into the cell. *Nature* 422: 37–44.
5. Belting M (2003) Heparan sulfate proteoglycan as a plasma membrane carrier. *Trends Biochem Sci* 28:145–151.
6. Sandvig K, Torgersen ML, Raa HA, van Deurs B (2008) Clathrin-independent endocytosis: From nonexisting to an extreme degree of complexity. *Histochem Cell Biol* 129:267–276.
7. Hill MM, et al. (2008) PTRF-Cavin, a conserved cytoplasmic protein required for caveola formation and function. *Cell* 132:113–124.
8. Parton RG, Simons K (2007) The multiple faces of caveolae. *Nat Rev Mol Cell Biol* 8: 185–194.
9. Takamori S, et al. (2006) Molecular anatomy of a trafficking organelle. *Cell* 127: 831–846.
10. Blondeau F, et al. (2004) Tandem MS analysis of brain clathrin-coated vesicles reveals their critical involvement in synaptic vesicle recycling. *Proc Natl Acad Sci USA* 101: 3833–3838.
11. Belting M, et al. (2002) Tumor attenuation by combined heparan sulfate and polyamine depletion. *Proc Natl Acad Sci USA* 99:371–376.
12. Mislick KA, Baldeschwieler JD (1996) Evidence for the role of proteoglycans in cation-mediated gene transfer. *Proc Natl Acad Sci USA* 93:12349–12354.
13. Wittrup A, et al. (2009) ScFv antibody-induced translocation of cell-surface heparan sulfate proteoglycan to endocytic vesicles: Evidence for heparan sulfate epitope specificity and role of both syndecan and glypican. *J Biol Chem* 284:32959–32967.
14. VanBuskirk AM, DeNagel DC, Guagliardi LE, Brodsky FM, Pierce SK (1991) Cellular and subcellular distribution of PBP72/74, a peptide-binding protein that plays a role in antigen processing. *J Immunol* 146:500–506.
15. Kaul SC, Aida S, Yaguchi T, Kaur K, Wadhwa R (2005) Activation of wild type p53 function by its mortalin-binding, cytoplasmically localizing carboxyl terminus peptides. *J Biol Chem* 280:39373–39379.
16. Mizukoshi E, et al. (1999) Fibroblast growth factor-1 interacts with the glucose-regulated protein GRP75/mortalin. *Biochem J* 343:461–466.
17. Kim KB, et al. (2006) Oxidation-reduction respiratory chains and ATP synthase complex are localized in detergent-resistant lipid rafts. *Proteomics* 6:2444–2453.
18. Chadda R, et al. (2007) Cholesterol-sensitive Cdc42 activation regulates actin polymerization for endocytosis via the GEEC pathway. *Traffic* 8:702–717.
19. Sandgren S, Cheng F, Belting M (2002) Nuclear targeting of macromolecular polyanions by an HIV-Tat derived peptide. Role for cell-surface proteoglycans. *J Biol Chem* 277:38877–38883.
20. Roghani M, Moscatelli D (1992) Basic fibroblast growth factor is internalized through both receptor-mediated and heparan sulfate-mediated mechanisms. *J Biol Chem* 267: 22156–22162.
21. Zong F, et al. (2009) Syndecan-1 and FGF-2, but not FGF receptor-1, share a common transport route and co-localize with heparanase in the nuclei of mesenchymal tumor cells. *PLoS ONE* 4:e7346.
22. Wadhwa R, Taira K, Kaul SC (2002) An Hsp70 family chaperone, mortalin/mthsp70/PBP74/Grp75: What, when, and where? *Cell Stress Chaperones* 7:309–316.
23. Shin BK, et al. (2003) Global profiling of the cell surface proteome of cancer cells uncovers an abundance of proteins with chaperone function. *J Biol Chem* 278: 7607–7616.
24. Lewis MJ, Pelham HR (1992) Ligand-induced redistribution of a human KDEL receptor from the Golgi complex to the endoplasmic reticulum. *Cell* 68:353–364.
25. Altmeyer A, et al. (1996) Tumor-specific cell surface expression of the-KDEL containing, endoplasmic reticular heat shock protein gp96. *Int J Cancer* 69:340–349.
26. Robert J, Ménoret A, Cohen N (1999) Cell surface expression of the endoplasmic reticular heat shock protein gp96 is phylogenetically conserved. *J Immunol* 163: 4133–4139.
27. Thériault JR, Mambula SS, Sawamura T, Stevenson MA, Calderwood SK (2005) Extracellular HSP70 binding to surface receptors present on antigen presenting cells and endothelial/epithelial cells. *FEBS Lett* 579:1951–1960.
28. Vega VL, et al. (2008) Hsp70 translocates into the plasma membrane after stress and is released into the extracellular environment in a membrane-associated form that activates macrophages. *J Immunol* 180:4299–4307.
29. Hwang EM, et al. (2007) Alternative splicing generates a novel non-secretable cytosolic isoform of NELL2. *Biochem Biophys Res Commun* 353:805–811.
30. Unoki M, Shen JC, Zheng ZM, Harris CC (2006) Novel splice variants of ING4 and their possible roles in the regulation of cell growth and motility. *J Biol Chem* 281: 34677–34686.
31. Pyhtila B, et al. (2008) Signal sequence- and translation-independent mRNA localization to the endoplasmic reticulum. *RNA* 14:445–453.
32. Varki A (2007) Glycan-based interactions involving vertebrate sialic-acid-recognizing proteins. *Nature* 446:1023–1029.
33. Glebov OO, Bright NA, Nichols BJ (2006) Flotillin-1 defines a clathrin-independent endocytic pathway in mammalian cells. *Nat Cell Biol* 8:46–54.

CELL BIOLOGY

Wittrup et al.